

# Micellization of Polystyrene-*b*-Poly(ethylene/butylene)-*b*-Polystyrene Triblock Copolymers in 4-Methyl-2-pentanone

Manuel Villacampa, José R. Quintana, R. Salazar, and Issa Katime\*

Grupo de Nuevos Materiales, Departamento de Química Física, Facultad de Ciencias, Universidad del País Vasco, Apartado 644, 48080 Bilbao, Spain

Received January 6, 1994; Revised Manuscript Received November 14, 1994\*

**ABSTRACT:** The micellization thermodynamics, micelle structural parameters, and micelle size distribution for polystyrene-*b*-poly(ethylene/butylene)-*b*-polystyrene copolymer solutions in 4-methyl-2-pentanone were studied. The solvent used is selective for the outer PS blocks of the copolymer. Standard Gibbs energy, standard enthalpy, and standard entropy of micellization were determined from light scattering measurements. The influence of the copolymer molar mass on these magnitudes was analyzed. The structural parameters of micelles formed by different triblock copolymers were determined by static light scattering. Micelle molar mass and size increase with the length of the copolymer chain for a constant copolymer composition; however the association number decreases. Micelle size distribution functions were obtained from dynamic light scattering and size exclusion chromatography measurements. The results obtained by means of both techniques were compared.

## Introduction

It is well-known that when a block copolymer of AB or ABA type is dissolved in a selective organic solvent which is a thermodynamically good solvent for one of the blocks and precipitant for the other, the block copolymer may associate in solution to form micelles as a result of different solvation of the copolymer blocks and their incompatibility.<sup>1–4</sup> The micelles consist of a relatively compact core formed by the least soluble blocks surrounded by a flexible and highly swollen shell formed by the other blocks. In most cases, these micelles have spherical shapes and narrow size distributions,<sup>5–7</sup> suggesting that micellization of block copolymers follows the closed association model,<sup>8</sup> which assumes a dynamic equilibrium between free copolymer chains and particles with an association number *n* (micelles).

According to this model, the critical micelle concentration, CMC, is defined as the concentration at which the experimental method in use can just detect the presence of micelles in the solution when the concentration is increased at constant temperature. At concentrations above the critical micelle concentration, all the copolymer chains added to the solution associate to form polymolecular associations (micelles).

A thermodynamic study of micelle formation can be carried out from the temperature dependence of the critical micelle concentration. For block copolymer systems with a high enough association number and a low micelle concentration, the standard Gibbs energy per mole of copolymer chain in the micellization process,  $\Delta G^\circ$ , can be expressed by

$$\Delta G^\circ \approx RT \ln \text{CMC} \quad (1)$$

If the association number does not depend on temperature, it follows from the above equation and the Gibbs–Helmholtz equation

$$\Delta H^\circ \approx R \frac{d \ln \text{CMC}}{dT^{-1}} \quad (2)$$

This equation allows us to determine the standard enthalpy of micellization,  $\Delta H^\circ$ . The standard entropy of micellization,  $\Delta S^\circ$ , can be calculated from the standard enthalpy and Gibbs energy.

The factors that influence the micellization process and the structural parameters of micelles include composition, structure, and molar mass of the copolymer, interactions between the copolymer blocks and the solvent, copolymer concentration, temperature, and preparation methods. Many studies on the characterization of micelle solutions have been carried out in recent years. However few of them have paid attention to the effect of the length of the copolymer block on the aggregation number and dimensions of the micelles<sup>9–14</sup> and on the thermodynamic behavior<sup>6,15,16</sup> for dilute solutions of block AB copolymers, and even fewer for solutions of block ABA copolymer.

The aim of the present paper is to analyze the thermodynamics of micelle formation and the structural parameters of micelles as a function of the molar mass of block copolymers of ABA type. The investigation was carried out for three polystyrene-*b*-poly(ethylene/butylene)-*b*-polystyrene copolymers, SEBS, in 4-methyl-2-pentanone. The three block copolymers have similar weight percentages of polystyrene but different molar masses. 4-Methyl-2-pentanone is a good solvent for the polystyrene blocks and a precipitant for the poly(ethylene/butylene) one.

## Experimental Section

**Materials.** Polystyrene-*b*-poly(ethylene/butylene)-*b*-polystyrene triblock copolymer (PS-*b*-PEB-*b*-PS) samples used—designated SEBS1, SEBS2, and SEBS3—are commercial products kindly provided by Shell España, S.A. Weight average molar masses of the three copolymers were determined by static light scattering in tetrahydrofuran, THF, and chloroform at 25 °C. The values obtained are shown in Table 1. The differences of molar masses of the three copolymers in both solvents were smaller than the experimental errors (3%). As both solvents and copolymer blocks have different refractive indices (1.403 THF; 1.447 chloroform; 1.59 polystyrene; 1.49 poly(ethylene/butylene)), these copolymers can be considered

\* Abstract published in *Advance ACS Abstracts*, January 15, 1995.

**Table 1. Characteristics of the Block Copolymers: Weight Average Molar Mass of the Copolymer,  $M_w$ , of the Polystyrene Blocks,  $M_{w,PS}$ , and of the Poly(ethylene/butylene) Block,  $M_{w,PB}$ , Polystyrene Weight Percentage, and Polydispersity Index,  $I$**

	SEBS1	SEBS2	SEBS3
$M_w/\text{g}\cdot\text{mol}^{-1}$	60 700	87 300	260 000
$M_{w,PS}/\text{g}\cdot\text{mol}^{-1}$	$2 \times 9100$	$2 \times 14000$	$2 \times 39000$
$M_{w,PB}/\text{g}\cdot\text{mol}^{-1}$	42 500	59 400	182 000
% PS by weight	30	32	30
$I$	1.09	1.11	1.18

homogeneous in chemical composition. The ratio weight average to number average molar mass,  $I$ , of the copolymers was determined by size exclusion chromatography (SEC) at 25 °C using THF as the solvent and a standard polystyrene calibration. UV spectroscopy measurements in THF were carried out to determine the weight PS percentage in the copolymers. The results are shown in Table 1.

4-Methyl-2-pentanone (Fluka, analytical purity grade, >99%) was used without further purification. The solvent used for light scattering measurements was filtered four times using 0.02  $\mu\text{m}$  aluminum oxide membrane filters (Anopore). All the solutions were prepared by dissolving the copolymer in the ketone at temperatures higher than 70 °C. This heating process was repeated before every measurement to obtain reproducible results. In order to clarify copolymer solutions for static and dynamic light scattering measurements, they were filtered at room temperature directly into the scattering cells using 0.2  $\mu\text{m}$  PTFE Acrodisc CR filters (Gelman Scientific). Then the cells were sealed. For the viscosity measurements, solutions were filtered with number 3 glass filters. Solution concentrations used to determine critical micelle temperatures, CMT, were recalculated at these CMTs. As all the used copolymer solutions are diluted, solutions were assumed to have the same thermal expansion coefficient as that of the pure solvent. The ketone used for SEC measurements was previously filtered and degassed. PTFE membranes with 0.45  $\mu\text{m}$  of pore diameter (Millipore) were employed for the filtration of the SEC solvent and solutions.

**Static Light Scattering.** Static light scattering measurements (SLS) were performed on a modified FICA 42000 light scattering photogoniometer. Both the light source and optical block of the incident beam were replaced by a Spectra-Physics He-Ne laser, Model 105, which emits vertically polarized light at 632.8 nm with a power of 5 mW. The instrument was calibrated with pure benzene by taking the Rayleigh ratio at 25 °C as  $12.55 \times 10^{-6} \text{ cm}^{-1}$ . This technique was used in order to determine thermodynamic parameters of the micellization process and the structure of micelles.

Investigations of the thermodynamics of micellization of block copolymers in organic solvents have shown that it is far better experimentally to carry out measurements in which the concentration is kept constant and the scattered light intensity is monitored over a range of temperatures in order to find the critical micelle temperature, CMT, than to keep the temperature constant and vary the concentration so as to find the critical micelle concentration.<sup>4,6</sup> The critical micelle temperature of a solution at a given concentration is the temperature at which the formation of micelles can just be detected experimentally.

Therefore, for block copolymers in organic solvents it has been shown<sup>17</sup> that, within experimental error

$$\frac{d \ln(\text{CMC})}{dT^{-1}} = \frac{d \ln(c)}{d(\text{CMT})^{-1}} \quad (3)$$

Thus, eq 2 becomes

$$\Delta H^\circ \approx R \frac{d \ln(c)}{d(\text{CMT})^{-1}} \quad (4)$$

To establish critical micelle temperatures, measurements of light scattered intensity were made at a series of temperatures within the range 25–90 °C at a scattering angle of 45°.

In order to get classical Zimm plots, light scattering measurements were taken at ten angles between 37.5 and 150° for the solvent and each copolymer solution at 25 °C. The light scattered by a dilute polymer solution may be expressed as<sup>18</sup>

$$\frac{Kc}{\Delta R(\theta)} = \frac{1}{M_w} \left( 1 + \frac{16\pi^2 n_0^2 R_G^2}{3\lambda_0^2} \sin^2(\theta/2) + \dots \right) + 2A_2c + \dots \quad (5)$$

where  $K$  is an optical constant,  $c$  is the polymer concentration,  $\Delta R(\theta)$  is the difference between the Rayleigh ratio of the solution and that of the pure solvent,  $M_w$  is the weight average molar mass,  $R_G^2$  is the mean square radius of gyration,  $n_0$  is the solvent refractive index,  $\lambda_0$  is the wavelength in vacuum, and  $A_2$  is the second virial coefficient.

**Refractive Index Increment.** To estimate  $M_w$  and  $R_G$ , it is necessary to know the refractive index increments,  $dn/dc$ , and the solvent refractive index,  $n_0$ . The refractive index increments of the copolymer solutions were measured using a Brice-Phoenix differential refractometer equipped with a He-Ne laser as the light source (Spectra-Physics, Model 156, 632.8 nm and power of 1 mW). The differential refractometer was calibrated with solutions of highly purified NaCl. The refractive indices of solvents were measured in an Abbé refractometer. The  $dn/dc$  values of SEBS3 copolymer in the different solvents used were 0.069 (chloroform), 0.1065 (THF), and 0.117 (4-methyl-2-pentanone).

**Viscometry.** Viscosity measurements were made in a Lauda automatic Ubbelohde viscometer Model Viscoboy 2, which was placed in a thermostatically controlled bath with a precision of  $\pm 0.01$  °C. The viscometer was calibrated using several standard solvents (*n*-dodecane, cyclohexane, water, toluene, ethyl acetate, acetone, and chloroform). Kinetic energy corrections were carried out by means of the equation

$$\eta = Aqt - \frac{Bq}{t} \quad (6)$$

where  $q$  is the density of the liquid,  $t$  is the efflux time, and  $A$  and  $B$  are the calibration constants ( $A = 1.016 \times 10^{-4} \text{ cm}^2\cdot\text{s}^{-2}$  and  $B = 4.3 \times 10^{-3} \text{ cm}^2$ ). Measurements of copolymer solutions were carried out within the polymer concentration range  $2 \times 10^{-3} \leq c \leq 5 \times 10^{-3} \text{ g}\cdot\text{cm}^{-3}$ . The data were evaluated according to Huggins<sup>19</sup> and Kraemer<sup>20</sup> equations

$$\frac{\eta_{sp}}{c} = [\eta] + k_1 [\eta]^2 c \quad (7)$$

$$\frac{\ln \eta_r}{c} = [\eta] - k_1' [\eta]^2 c \quad (8)$$

$c$  being the polymer concentration,  $\eta_{sp}$  the specific viscosity,  $\eta_r$  the viscosity ratio,  $[\eta]$  the intrinsic viscosity, and  $k_1$  and  $k_1'$  the Huggins and Kraemer coefficients, respectively.

**Dynamic Light Scattering.** DLS measurements were carried out in a PL-LSP-700 instrument (Polymer Laboratories) working in the dynamic homodyne mode. The autocorrelation functions  $g^{(2)}(\tau)$ , where  $\tau$  is the delay time, were obtained and analyzed in a personal computer by means of the software PL-LSP. These  $g^{(2)}(\tau)$  functions are transformed in the electric field autocorrelation function,  $g^{(1)}(\tau)$ . In order to get the translational diffusion coefficient and structural information of the copolymer solutions, two calculation methods (both supplies by the software package) were used: (a) The second order cumulants method, which gives the translational diffusion coefficient,  $D$ , the average line width,  $\bar{\Gamma}$ , and the variance of the size distribution function,  $\mu_2/\bar{\Gamma}^2$ . In order to get this information, the cumulants expansion method<sup>21</sup> is applied

$$\log[g^{(1)}(\tau)] = -\bar{\Gamma}\tau + \frac{1}{2}\mu_2\tau^2 \quad (9)$$

(b) The histogram method,<sup>22</sup> which consists of the decomposition of  $g^{(1)}(\tau)$  in a sum of single exponential functions,

$$g^{(1)}(\tau) = \sum_{i=1}^N G_i \exp(-\bar{\Gamma}_i \tau) \quad (10)$$

where  $N$  is the number of steps in the histogram,  $G_i$  is the total integrated intensity scattered by all the species  $i$  that contribute to the amplitude of the  $\Gamma_i$  increment from  $\Gamma_i - \Delta\Gamma/2$  to  $\Gamma_i + \Delta\Gamma/2$  (being  $\Delta\Gamma = (\Gamma_{\max} - \Gamma_{\min})/N$  the width of each step) and  $\bar{\Gamma}_i$  is the average value of  $\Gamma$  in the  $\Gamma_i$  increment. We chose a Gaussian distribution function to fit the experimental correlation function, selecting lower and higher limits far enough from the values of the micelles to avoid errors in the calculation. This process allows us to get the  $z$ -weighted size distribution function of the particles.

Once  $\Gamma$  has been obtained (by any of the two methods), the translational diffusion coefficient,  $D$ , and the hydrodynamic radius (the average value with the cumulants method or each fraction value for the histogram one) can be obtained from the equation

$$\Gamma = DK^2 \quad (11)$$

$$K = \left( \frac{4\pi n_0}{\lambda_0} \sin\left(\frac{\theta}{2}\right) \right) \quad (12)$$

and the Stokes-Einstein relation

$$D_0 = \frac{k_B T}{6\pi\eta_0 R_h} \quad (13)$$

where  $D_0$  is the translational diffusion coefficient extrapolated to nil concentration,  $K$  is the scattering vector,  $\theta$  is the angle of scattering,  $\lambda_0$  is the vacuum wavelength,  $n_0$  is the refractive index of the medium,  $k_B$  is Boltzmann's constant,  $T$  is the absolute temperature,  $\eta_0$  is the viscosity of the solvent, and  $R_h$  is the particle hydrodynamic radius.

From the  $z$ -weighted size distribution function of the particles, the weight size distribution function was determined by using the approximation  $D \propto M^{-1/3}$ .

All the experiments were carried out for solutions of  $1 \times 10^{-3} \text{ g cm}^{-3}$  at  $25^\circ\text{C}$ , at an observation angle of  $90^\circ$  with a delay time of  $1024 \mu\text{s}$  (128 channels and  $8 \mu\text{s}/\text{data}$ ) and by averaging 500 measurements. Previous measures demonstrated that the values obtained at different angles ( $30^\circ$ ,  $90^\circ$ , and  $150^\circ$ ) and at concentrations lower than  $2 \times 10^{-3} \text{ g cm}^{-3}$  led to identical results. Therefore, it is not necessary to extrapolate to null concentration or angle, as it has been reported previously in the literature for other micellar systems.<sup>23</sup>

**Size Exclusion Chromatography.** Size exclusion chromatography measurements, SEC, were carried out in a home-built instrument constituted by a piston pump Gilson 303, a manometric module Gilson 802C, a Rheodyne injector provided with a  $100 \mu\text{L}$  loop, three chromatographic columns ( $250 \text{ mm}$  long, i.d.  $4 \text{ mm}$ , packed with Nucleosil silica gel with a  $5 \mu\text{m}$  particle diameter and pore sizes of 4000, 1000, and  $500 \text{ \AA}$ ), and a refraction index detector Waters R401. Columns were placed in a thermostatically controlled bath. The refraction index detector was also thermostatically controlled. All measurements were carried out at solvent flux of  $1 \text{ mL min}^{-1}$  at  $25^\circ\text{C}$ .

## Results and Discussion

Relationships of concentration and CMT for the copolymers SEBS1 and SEBS2 in 4-methyl-2-pentanone were determined. For SEBS3, only the CMT corresponding to a solution of concentration  $1.5 \times 10^{-5} \text{ g cm}^{-3}$  was determined, its value being  $85^\circ\text{C}$  (the highest temperature that our experimental device can determine). Thus, the standard Gibbs energy of micellization corresponding to the block copolymer SEBS3 in 4-methyl-2-pentanone at this temperature is  $-49.5 \text{ kJ mol}^{-1}$ . In Figure 1, the light scattering intensity

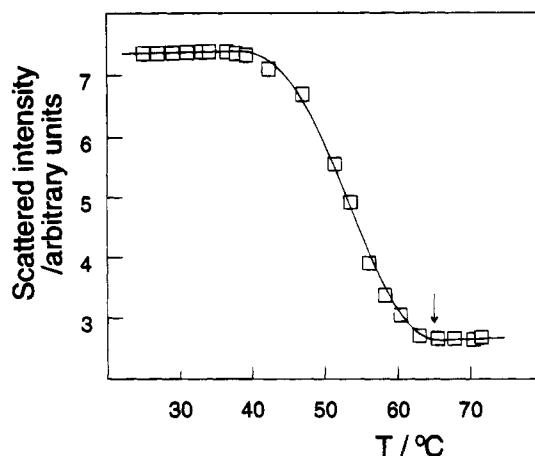


**Figure 1.** Temperature dependence of the scattered light intensity at  $45^\circ$  for a SEBS1 solution ( $c = 4 \times 10^{-3} \text{ g cm}^{-3}$ ) in 4-methyl-2-pentanone. The arrow indicates the critical micelle temperature.

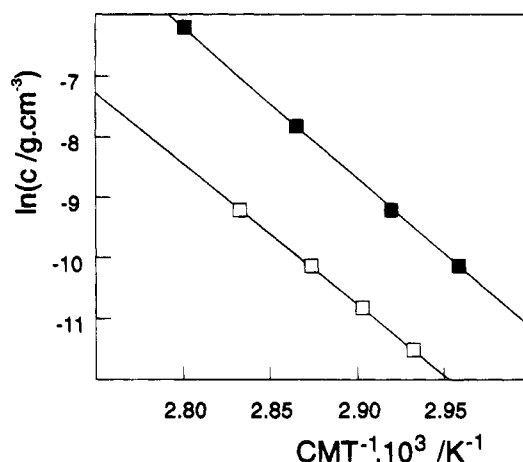


**Figure 2.** Plots of  $\ln(c)$  as a function of the reciprocal of the critical micellar temperature for solutions of SEBS1 (■) and SEBS2 (□) copolymers in 4-methyl-2-pentanone.

measured at the observation angle of  $45^\circ$  is plotted as a function of temperature for copolymer SEBS1 in 4-methyl-2-pentanone at a concentration of  $4 \times 10^{-5} \text{ g cm}^{-3}$ . The influence of temperature on the equilibrium between micelles and free chains controls the shape of the plot. At low temperatures the equilibrium is overwhelmingly in favor of micelle formation whereas at the upper end of the temperature range studied only free chains exist in the solution. On lowering the temperature from a high value, an abrupt increase in the scattered intensity is observed due to the appearance of micelles. Similar curves  $I = f(T)$  have been found when the temperature is increased and decreased for all systems studied. The temperature at which the presence of micelles in the solution have just been detected was considered as the critical micelle temperature.

CMTs were determined for SEBS1 and SEBS2 solutions covering a range of concentrations between  $1 \times 10^{-5}$  and  $2 \times 10^{-3} \text{ g cm}^{-3}$  in 4-methyl-2-pentanone. All the plots are similar to the one shown in Figure 1. Plots of  $\ln(c)$  as a function of  $(\text{CMT})^{-1}$  for solutions of copolymers SEBS1 and SEBS2 in 4-methyl-2-pentanone are shown in Figure 2. Both are linear within experimental error for the temperature range studied.

The standard Gibbs energy,  $\Delta G^\circ$ , at  $25$  and  $85^\circ\text{C}$ , the standard enthalpy,  $\Delta H^\circ$ , and the standard entropy of micellization,  $\Delta S^\circ$ , were calculated from the experimen-

**Table 2. Thermodynamic Data for the Micellization Process of Copolymers SEBS in 4-Methyl-2-pentanone**

	SEBS1	SEBS2	SEBS3
$\Delta H^\circ/\text{kJ}\cdot\text{mol}^{-1}$	-216	-204	
$\Delta S^\circ/\text{kJ}\cdot\text{mol}^{-1}\cdot\text{K}^{-1}$	-0.520	-0.454	
$\Delta G^\circ_{25}/\text{kJ}\cdot\text{mol}^{-1}$	-60.1	-68.6	
$\Delta G^\circ_{85}/\text{kJ}\cdot\text{mol}^{-1}$	-30.5	-41.3	-49.5
$\text{CMC}_{25}/\text{g}\cdot\text{cm}^{-3}$	$9.5 \times 10^{-10}$	$8.2 \times 10^{-11}$	
$\text{CMC}_{25}/\text{mol}\cdot\text{L}^{-1}$	$1.6 \times 10^{-11}$	$9.4 \times 10^{-13}$	
$\text{CMC}_{85}/\text{g}\cdot\text{cm}^{-3}$	$2.1 \times 10^{-3}$	$8.2 \times 10^{-5}$	$1.5 \times 10^{-5}$
$\text{CMC}_{85}/\text{mol}\cdot\text{L}^{-1}$	$3.5 \times 10^{-5}$	$9.4 \times 10^{-7}$	$5.8 \times 10^{-8}$

tal data by means of eqs 1–4. These values, per mole of copolymer chain, are shown in Table 2. The standard states for micelles and chains are states with ideally dilute solution behavior and concentration  $1 \text{ mol}\cdot\text{dm}^{-3}$ . It was assumed that  $\Delta H^\circ$  and  $\Delta S^\circ$  were independent of temperature from 25 to 85 °C in order to calculate  $\Delta G^\circ$  at 25 °C.

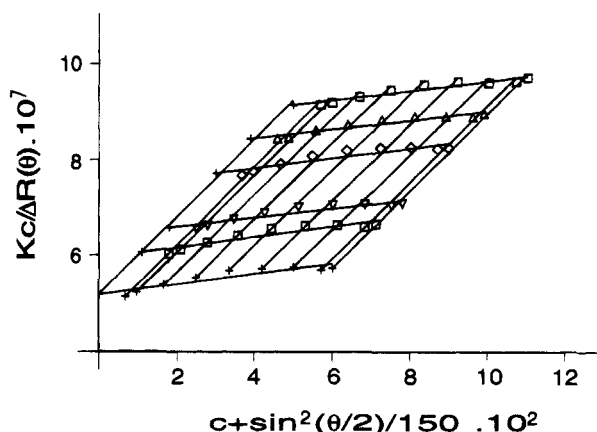
The standard Gibbs energy of micellization shows negative values for all the studied systems, as expected. As can be seen in Table 2, when the copolymer molar mass is increased, the standard Gibbs energy becomes more negative. So, the stability of micelle solutions is higher for larger copolymer chains.

The standard enthalpy of micellization also shows negative values and is solely responsible of the micelle formation. These negative values arise from the exothermic energy interchange which accompanies the replacement of core block segment/solvent interactions by core block segment/core block segment and solvent/solvent interactions in the formation of the micelle cores. Values of  $\Delta H^\circ$  are similar for the copolymers SEBS1 and SEBS2, which can be explained by taking into account the small difference between their PEB blocks.

The standard entropy of micellization is also negative in all the systems and, therefore, unfavorable to the micellization process. The negative values of the standard entropy of micellization are due to the increase of the order degree that is associated with the micellization process. As can be seen in Table 2, SEBS1 micelles have a more negative  $\Delta S^\circ$  value than SEBS2 micelles, although the molar mass of the first micelles are smaller than the second ones. This fact can be explained by considering the higher associating number that SEBS1 micelles have and the influence of this parameter in the order degree.

In order to study the micelle structure, static and dynamic light scattering, size exclusion chromatography, and viscometry techniques were employed. Static light scattering measurements were performed on solutions of the three copolymers whose concentrations range between  $1 \times 10^{-3}$  and  $5 \times 10^{-3} \text{ g}\cdot\text{cm}^{-3}$ . The Zimm plots obtained show a standard shape (Figure 3) since the experimental concentrations are very much higher than the critical micelle concentration (Table 2). Under these experimental conditions micelle formation is overwhelmingly favored and the weight average molar mass,  $M_w$ , determined from the double extrapolation to nil angle and concentration can be considered as the micelle molar mass (Table 3).

As shown in Table 3, the molar mass of the micelles increases as the molar mass of the copolymer becomes higher. However, the association number has an opposite behavior, decreasing with the copolymer molar mass. This behavior agrees with the variation of the standard entropy of micellization with the copolymer molar mass. This fact can be explained by considering that as the copolymer chain becomes larger, its arrange-

**Figure 3.** Zimm plot for micellar solutions of SEBS3 copolymer in 4-methyl-2-pentanone at 25 °C.**Table 3. Molar Mass,  $M_w$ , Association Number,  $N$ , Second Virial Coefficient,  $A_2$ , Mean Square Radius of Gyration,  $R_G$ , Intrinsic Viscosity,  $[\eta]$ , Degree of Solvation,  $\xi$ , and Hydrodynamic Radius (Obtained from Static Light Scattering and Viscosimetric Measurements),  $R_h$ , for SEBS Copolymer Micelles in 4-Methyl-2-pentanone**

	SEBS1	SEBS2	SEBS3
$10^{-6}M_w/\text{g}\cdot\text{mol}^{-1}$	9.5	10	21
$N$	157	115	81
$10^6A_2/\text{mol}\cdot\text{cm}^3\cdot\text{g}^{-2}$	1.2	0.6	4.6
$R_G/\text{nm}$	16.0	16.0	23.9
$[\eta]/\text{cm}^3\cdot\text{g}^{-1}$	8.54	9.05	13.40
$\xi$	1.89	2.05	3.44
$R_h/\text{nm}$	23.4	24.3	35.5

ment into the micelle is more difficult. In all cases, the association numbers are considerably lower than those found in ketones for SEP diblock copolymers with similar PS contents<sup>12,24</sup> (around 400 molecules per micelle). This fact agrees with that found by Riess and Roger<sup>25</sup> for diblock and triblock copolymers of polystyrene and poly(ethylene oxide). PEP insoluble blocks of SEP diblock copolymers can be packed more easily into the micelle core than the PEB central blocks of SEBS triblock copolymers since the two lateral blocks hinder sterically the association of the central block.

Second virial coefficients,  $A_2$ , were determined from the concentration dependence of  $Kc/\Delta R$  at nil angle. In all cases the second virial coefficient showed small and positive values (Table 3), which can be explained by taking into account that the solvent is rejected from the micelle core giving rise to less unfavorable contacts between the PEB segment and the 4-methyl-2-pentanone molecules. On the other hand, the protective shell of solvated PS segments hinders long-range PEB segment–PEB segment interactions.

The radius of gyration,  $R_G$ , has been calculated from the angle dependence of  $Kc/\Delta R$  at nil concentration. The values are shown in Table 3. Owing to the micelle structure and the different refractive index increments that PS and PEB segments have, the experimental radii of gyration are apparent. Besides, the  $R_G$  values found are in the experimental low limit of the static light scattering technique; therefore they must be considered in a qualitative way. Block copolymer micelles show very small dimensions when compared to free polymer chains. Thus a PS sample with a weight average molar mass of  $1.05 \times 10^6 \text{ g}\cdot\text{mol}^{-1}$  shows a radius of gyration of 30.0 nm in 4-methyl-2-pentanone at 25 °C. Taking into account the high molar mass that the micelles have (several millions), the low values of  $R_G^*$  suggest a very

high compactness, mainly due to the high density of the micelle core.

Viscometry measurements were carried out in order to get the intrinsic viscosity,  $[\eta]$ , the hydrodynamic radius,  $R_h$ , and the solvation degree,  $\xi$ . The experimental dependencies of the reduced viscosity,  $\eta_{sp}/c$  (Huggins equation), and of the logarithm viscosity number,  $\ln(\eta_r/c)$  (Kraemer equation), on the concentration were linear within the concentration range employed for the three SEBS/4-methyl-2-pentanone systems analyzed. Extrapolations to nil concentration according to the Huggins and Kraemer equations led to the same values of  $[\eta]$  (see Table 3). These intrinsic viscosities correspond to the micelle ones. The molar mass of PS samples which would correspond to these intrinsic viscosity values ( $1.2 \times 10^4$ ,  $1.3 \times 10^4$ , and  $2.8 \times 10^4$  g·mol<sup>-1</sup>) were calculated by means of the Mark-Houwink-Sakurada relationship for the system polystyrene/4-methyl-2-pentanone/25 °C. These values are very much lower than the ones of the micelles ( $9.5 \times 10^6$ ,  $1.0 \times 10^7$ , and  $2.1 \times 10^7$  g·mol<sup>-1</sup>). Therefore the very low  $[\eta]$  values found give a qualitative idea of the high compactness of the micelle core and confirm the small  $R_G^*$  values obtained by static light scattering, considering the high molar mass that the micelles have. The values of the Huggins coefficient,  $K_1$ , found for the three systems are lower than 0.35. These values are similar to those found for solutions of a polystyrene-*b*-poly(ethylene/propene) diblock copolymer in several ketones<sup>12,24</sup> but contrast with the values shown for the same copolymer in *n*-alkanes<sup>12,26</sup> (ranged between 0.6 and 0.9). It can be explained by the higher density that the micelles formed by block copolymers with low polystyrene content have done so in polystyrene selective solvents. This fact decreases the intermicellar interactions and avoids the anomalous values of the Huggins coefficients and the negative slope of the angle dependence of  $Kc/\Delta R(\theta)$  that other micellar systems show at the same experimental concentrations.<sup>12,26</sup>

The hydrodynamic radius of the micelles was calculated from viscosity and SLS measurements by applying the model of the hydrodynamically equivalent sphere to the spherical micelles and using Einstein's equation

$$M[\eta] = \nu \frac{4\pi N_A R_h^3}{3} = \frac{10\pi N_A R_h^3}{3} \quad (14)$$

where  $\nu$  is the shape factor (2.5 for rigid spheres),  $M$  and  $R_h$  are the molar mass and the hydrodynamic radius of the micelles, and  $N_A$  is Avogadro's number. According to the above equation, the intrinsic viscosity is inversely proportional to the density of the micelles. Although the intrinsic viscosity is a viscosity average and the molar mass determined by light scattering is a weight average, both averages can be considered similar. The spherical micelles have a narrow size distribution, as size exclusion chromatography and dynamic light scattering measurements have shown.

The  $R_h$  values obtained are shown in Table 3. Very low values were found and provide a new evidence of the high density of micelles. The SEBS3 copolymer forms micelles larger than those formed by SEBS1 and SEBS2 copolymers. This can be explained by taking into account the higher molar mass of SEBS3 micelles and the larger solvated PS blocks that this copolymer has.

Information on the micellar shape can be obtained from the relationship radius of gyration versus hydrodynamic radius. It must be noted that the  $R_G^*/R_h$  ratio

**Table 4. Translational Diffusion Coefficient,  $D$ , Hydrodynamic Radius,  $R_h$ , and Variance,  $\mu_2/\Gamma^2$ , Determined by DLS (Cumulants Method) for SEBS Copolymer Micelles in 4-Methyl-2-pentanone**

	SEBS1	SEBS2	SEBS3
$10^7 D/\text{cm}^2\text{s}^{-1}$	1.673	1.593	1.186
$R_h/\text{nm}$	26.1	27.5	36.9
$\mu_2/\Gamma^2$	0.027	0.025	0.032

is constant for the three copolymer samples ( $R_G^*/R_h = 0.67 \pm 0.01$ ), suggesting that the micelles of the three samples have a similar shape. The theoretical ratio  $R_G/R_h$  is 0.77 for a hard sphere<sup>18</sup> and 1.30 for a linear coil.<sup>27</sup> Therefore, even considering the apparent character of the radii of gyration, the  $R_G^*/R_h$  values indicate that the assumption of considering the micelles as hydrodynamic hard spheres is acceptable.

The intrinsic viscosity is related to the degree of solvation  $\xi$  (weight of solvent within the micelle per weight of copolymer) by the equation

$$[\eta] = \nu/\rho^* = \nu(\rho_p^{-1} + \xi\rho_s^{-1}) \quad (15)$$

where  $\nu$  is the shape factor (2.5 for spheres) and  $\rho^*$ ,  $\rho_p$ , and  $\rho_s$  are the densities of the particle, polymer (0.96 g·cm<sup>-3</sup>), and solvent (0.80 g·cm<sup>-3</sup>), respectively.

Equation 15 allows us to determine the degree of solvation (Table 3). These  $\xi$  values must be considered average ones since the micelle core will be very much less solvated than the shell. The values calculated are similar to those found for micelles of nonionic surfactants in water.<sup>28</sup> Similarly to the second virial coefficient, the degree of solvation of SEBS3 shows a slightly higher value compared to those corresponding to SEBS1 and SEBS2. Taking into account that the core of SEBS3 micelles is larger and the association number is smaller, the PS blocks which form the shell of the SEBS3 micelles will have fewer steric hindrances. Therefore the shell of the SEBS3 micelles will be able to be more solvated.

Dynamic light scattering measurements were made in order to get information on the size distribution functions and to confirm the previous results. Parameters obtained by the cumulants method are shown in Table 4. As expected, these DLS hydrodynamic radii (*z*-average) are slightly higher than those calculated by SLS and viscometry (weight-average). The dependence of  $\ln(g^{(2)}(\tau) - 1)$  as a function of the delay time for the SEBS2 copolymer in 4-methyl-2-pentanone at 25 °C is shown in Figure 4. The plot is linear, leading to very low values of the variances ( $\mu_2/\Gamma^2 \leq 0.032$ ), which suggests a low particle size polydispersity.

The histograms method allows us to get the whole size distribution function and the different average hydrodynamic radii. Figure 5 shows the distribution histograms for the three SEBS/4-methyl-2-pentanone systems. The distribution functions are narrow and shift to high radius values as copolymer and micelle weights are increased. The values of the average hydrodynamic radii and polydispersity index obtained by DLS are shown in Table 5. Weight average values are similar to those obtained from SLS and viscosity measurements. The polydispersity indices are close to the unit and agree with the low values of the variance found by the cumulants method. These low values provide new proof of the existence of the closed association mechanism in the system.

Size exclusion chromatography measurements were also made. In order to determine the hydrodynamic

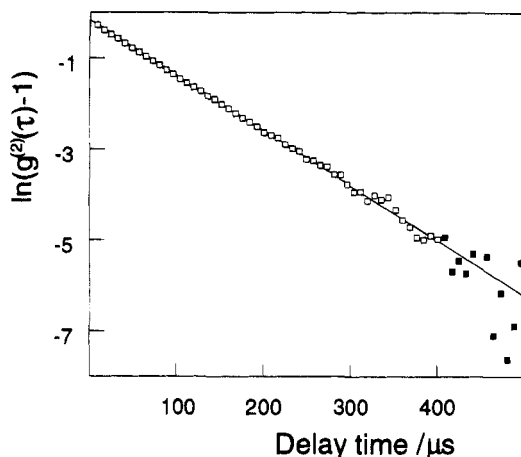


**Figure 4.** Plot of  $\ln(g^{(2)}(\tau) - 1)$  versus delay time for a SEBS2/4-methyl-2-pentanone solution with  $c = 1 \times 10^{-3} \text{ g cm}^{-3}$  at 25 °C.

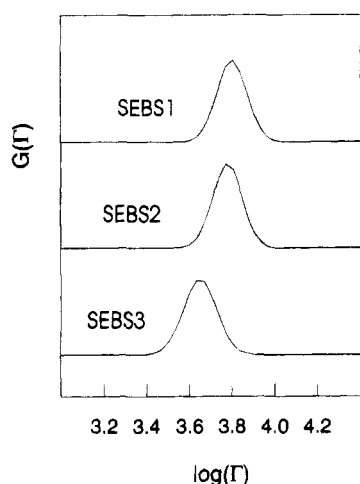


**Figure 5.** Plots of  $G(\Gamma)$  versus  $\log(\Gamma)$  for SEBS copolymers in 4-methyl-2-pentanone at 25 °C ( $c = 1 \times 10^{-3} \text{ g cm}^{-3}$ ).

**Table 5.** Polydispersity,  $I$ , and Different Values of the Hydrodynamic Radii (Chromatographic Peak Value,  $R_{h,peak}$ ; Number Average,  $R_{h,n}$ ; Weight Average,  $R_{h,w}$ ; and Z-Average,  $R_{h,z}$ ) of Micelles Obtained by SEC and DLS (Histogram Method) for SEBS/4-Methyl-2-pentanone Systems at 25 °C

	SEBS1		SEBS2		SEBS3	
	SEC	DLS	SEC	DLS	SEC	DLS
$R_{h,peak}/\text{nm}$	23.3		25.3		35.9	
$R_{h,n}/\text{nm}$	23.2	24.6	23.8	25.9	30.7	34.3
$R_{h,w}/\text{nm}$	23.6	24.9	24.2	26.2	31.7	34.9
$R_{h,z}/\text{nm}$	25.2	26.3	25.4	27.5	35.0	37.1
$I$	1.02	1.01	1.02	1.01	1.03	1.02

sizes of the micelles it was necessary to carry out a previous universal calibration. Therefore, the values of the Mark-Houwink-Sakurada coefficients for the system polystyrene/4-methyl-2-pentanone at 25 °C had to be determined from the  $\log[\eta]$  versus  $\log M$  relationship plotted in Figure 6 ( $K = 5.414 \times 10^{-2} \text{ cm}^3 \text{ g}^{-1}$ ,  $a = 0.539$ ). The universal calibration curve<sup>29</sup> was obtained from the dependence of  $\log(M[\eta])$  as a function of the elution volume,  $V_e$ , for the different polystyrene standard samples injected (Figure 7). The size distribution functions of micellar samples were directly determined from their chromatograms by means of the calibration curve. The value of the hydrodynamic radius of each fraction was obtained by taking into account the Einstein relationship for hydrodynamically equivalent spheres (eq 14).

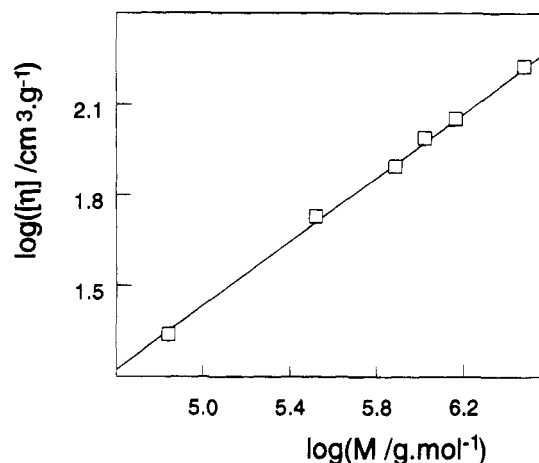


**Figure 6.** Plot of  $\log[\eta]$  versus  $\log M$  for several monodisperse polystyrene samples in 4-methyl-2-pentanone at 25 °C.

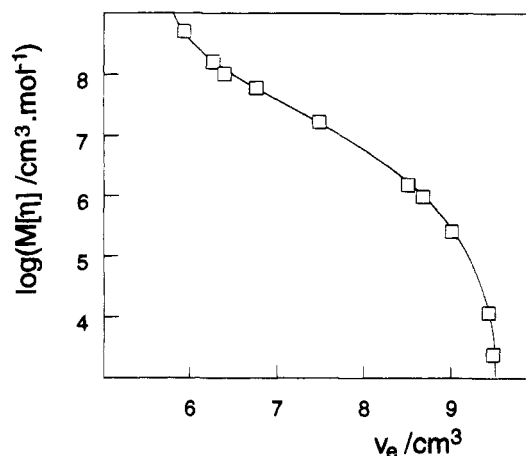


**Figure 7.** Plot of  $\log M[\eta]$  as a function of the elution volume,  $V_e$ , for several polystyrene samples in 4-methyl-2-pentanone at 25 °C.

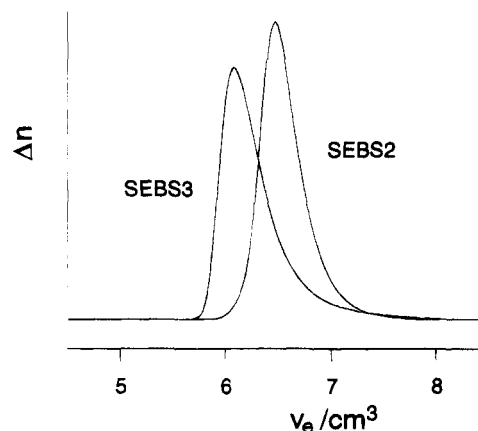


**Figure 8.** Chromatograms of SEBS2 and SEBS3 triblock copolymer micelles in 4-methyl-2-pentanone at 25 °C ( $c = 2 \times 10^{-3} \text{ g cm}^{-3}$ ).

The chromatograms corresponding to SEBS2 and SEBS3 copolymer micelles in 4-methyl-2-pentanone at 25 °C are shown in Figure 8. The micelle chromatograms have a small tail. This behavior contrasts with that shown for other micelle/solvent/temperature systems, whose peaks have a large tail.<sup>30,31</sup> The anomalous shape of these chromatograms is due to the continuous establishment of the association equilibrium in the column. When the copolymer elutes through the column, micelles are separated from unimers. In order to

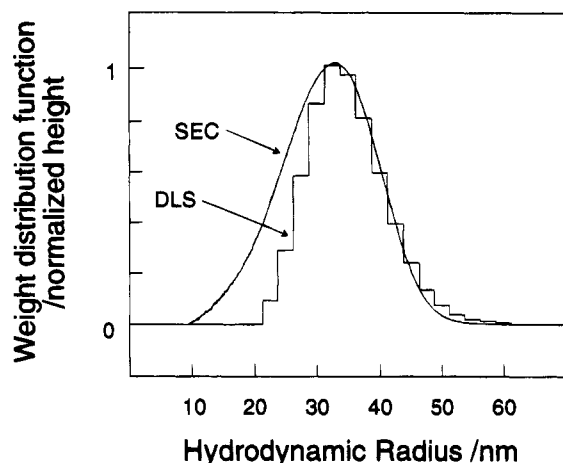


**Figure 9.** Particle size distribution functions obtained by SEC and DLS for the system SEBS3/4-methyl-2-pentanone at 25 °C.

recover the equilibrium, micelles dissociate along the column. This effect is more pronounced as the molecule interchange rate between unimers and micelles increases and as the critical micelle concentration becomes higher. The shape of the chromatograms of SEBS triblock copolymers (with small or no tail) suggests a slower speed in the dissociation process of triblock copolymer micelles in comparison with other micelle/solvent/temperature systems reported in the literature.<sup>32</sup>

Such behavior allows us to calculate the size distribution functions directly from the chromatograms of triblock copolymer micelles with a small error. The size distribution functions obtained by SEC and DLS for the system SEBS3/4-methyl-2-pentanone at 25 °C are compared in Figure 9. The results obtained for the three systems studied are shown in Table 5. All the average values are close to that given by DLS, only slightly smaller. This fact is due to the influence of the micellar equilibrium in the shape of the chromatographic peak and therefore in the size distribution functions evaluated from the SEC measurements. However, the effect of the micellization equilibrium on the results obtained is low and SEC can be considered as a valid method to characterize these triblock copolymer micelles. Although the polydispersity indices are higher than those obtained by DLS, they are extremely low and confirm the close association model and the validity of the SEC technique.

As shown in Table 5, peak location in the SEC curve can be considered as a good criterion to determine the hydrodynamic radius of triblock copolymer micelles, since micelles are practically monodisperse. These values are in good agreement with those obtained by other methods.

## Conclusions

Polystyrene-*b*-poly(ethylene/butylene)-*b*-polystyrene triblock copolymers form micelles in selective solvents of the external polystyrene blocks. The extremely low size polydispersities obtained by DLS and SEC suggest that the association process follows the closed association model. In order to explain the micellization process, thermodynamic arguments similar to those shown for diblock copolymers can be used, i.e. the enthalpy contribution is solely responsible for micelle formation, whereas the entropy contribution is unfavorable. The association numbers and solvation degrees found are

lower than those shown by diblock copolymers, as a consequence of the steric effect. Micelle molar mass and size increase as the copolymer chains become larger for a constant copolymer composition. However, the association number has an opposite behavior.

**Acknowledgment.** We thank Shell España, S.A., for the copolymer samples and CYTED (Programa Iberoamericano de Ciencia y Tecnología para el Desarrollo) and Vicerrectorado de Investigación of the Universidad del País Vasco (UPV/EHU) for financial support. R.S. thanks the Instituto de Cooperación Iberoamericana for a research fellowship.

## References and Notes

- (1) Tuzar, Z.; Kratochvíl, P. *Adv. Colloid Interface Sci.* **1976**, *6*, 201.
- (2) Brown, R. A.; Masters, A. J.; Price, C.; Yuan, X. F. In *Comprehensive Polymer Science*; Booth, C., Price, C., Eds.; Pergamon Press: Oxford, U.K., 1989; Vol. 2, Chapter 6, p 155.
- (3) Quintana, J. R.; Villacampa, M.; Katime, I. *Rev. Iberoam. Polím.* **1992**, *1*, 5.
- (4) Price, C. *Pure Appl. Chem.* **1983**, *55*, 1563.
- (5) Price, C.; Hudd, A. L.; Booth, C.; Wright, B. *Polymer* **1982**, *23*, 650.
- (6) Price, C.; Stubbersfield, R. B.; El-Kafrawy, S.; Kendall, K. D. *Br. Polym. J.* **1989**, *21*, 391.
- (7) Candau, F.; Heatley, F.; Price, C.; Stubbersfield, R. B. *Eur. Polym. J.* **1984**, *20*, 685.
- (8) Elias, H.-G. In *Light Scattering from Polymer Solutions*; Huglin, M. B., Ed.; Academic Press: London, 1972.
- (9) Oranli, L.; Bahadur, P.; Riess, G. *Can. J. Chem.* **1985**, *63*, 2691.
- (10) Bahadur, P.; Sastry, N. V.; Marti, S.; Riess, G. *Colloid Surf.* **1985**, *16*, 337.
- (11) Bluhm, T. L.; Malhotra, S. L. *Eur. Polym. J.* **1986**, *22*, 249.
- (12) Quintana, J. R.; Villacampa, M.; Katime, I. *Makromol. Chem.* **1993**, *194*, 983.
- (13) Xu, R.; Winnik, M. A.; Riess, G.; Chu, B.; Croucher, M. D. *Macromolecules* **1992**, *25*, 644.
- (14) Xu, R.; Winnik, M. A.; Hallett, F. R.; Riess, G.; Croucher, M. D. *Macromolecules* **1991**, *24*, 87.
- (15) Quintana, J. R.; Villacampa, M.; Salazar, R.; Katime, I. *J. Chem. Soc., Faraday Trans.* **1992**, *88*, 2739.
- (16) Price, C.; Chan, E. K. M.; Stubbersfield, R. B. *Eur. Polym. J.* **1987**, *23*, 649.
- (17) Price, C.; Booth, C.; Canham, P. A.; Naylor, T. V.; Stubbersfield, R. B. *Br. Polym. J.* **1984**, *16*, 311.
- (18) Katime, I.; Quintana, J. R. In *Comprehensive Polymer Science*; Booth, C., Price, C., Eds.; Pergamon Press: Oxford, U.K., 1989; Vol. 1.
- (19) Huggins, M. L. *J. Am. Chem. Soc.* **1942**, *64*, 2716.
- (20) Kraemer, E. O. *Ind. Eng. Chem.* **1938**, *30*, 1200.
- (21) Koppel, D. E. *J. Chem. Phys.* **1972**, *57*, 4814.
- (22) Gulari, Es.; Gulari, Erd.; Tsunashima, Y.; Chu, B. *J. Chem. Phys.* **1979**, *70*, 3965.
- (23) Price, C.; McAdam, J. D. G.; Lally, T. P.; Woods, D. *Polymer* **1974**, *15*, 228.
- (24) Quintana, J. R.; Villacampa, M.; Katime, I. *Polymer* **1993**, *34*, 2380.
- (25) Riess, G.; Rogez, D. *Polym. Prepr. (Am. Chem. Soc., Div. Polym. Chem.)* **1982**, *23* (1), 19.
- (26) Quintana, J. R.; Villacampa, M.; Andrio, A.; Muñoz, M.; Katime, I. *Macromolecules* **1992**, *25*, 3129.
- (27) Kuk, Ch.M.; Rudin, A. *Makromol. Chem., Rapid Commun.* **1981**, *2*, 665.
- (28) Elias, H.-G. *J. Macromol. Sci., Chem.* **1973**, *A7* (3), 601.
- (29) Benoit, H.; Grubisic, Z.; Rempp, P.; Decker, D.; Zilliox, J. G. *J. Chem. Phys.* **1966**, *11-12*, 1507.
- (30) Spacek, P.; Kubin, M. *J. Appl. Polym. Sci.* **1985**, *30*, 143.
- (31) Booth, C.; Naylor, T. D.; Price, C. *J. Chem. Soc., Faraday Trans. 1* **1978**, *74*, 2352.
- (32) Bednar, B.; Edwards, K.; Almgren, M.; Tormod, S.; Tuzar, Z. *Makromol. Chem. Rapid Commun.* **1988**, *9*, 785.